Optics Letters

Impact of the Coulomb interaction on the Franz–Keldysh effect in high-current photodetectors

Yue Hu,[1,*] Curtis R. Menyuk,[1] Meredith N. Hutchinson,[2] Vincent J. Urick,[2] and Keith J. Williams[2]

[1]University of Maryland, Baltimore County, 1000 Hilltop Circle, Baltimore, Maryland 21250, USA
[2]Naval Research Laboratory, Photonics Technology Branch, Washington, DC 20375, USA
*Corresponding author: yuehu1@umbc.edu

Received 17 September 2015; accepted 19 November 2015; posted 3 December 2015 (Doc. ID 250319); published 19 January 2016

The Franz–Keldysh effect has been recognized as the largest contributor to oscillations in the responsivity of high-current photodetectors as a function of the applied bias or the incident light wavelength and to device nonlinearity. Prior work only considered the effect of the electric field without considering the Coulomb interaction. We show that it is not possible to obtain agreement with experiments at all optical wavelengths without including this effect in the effective mass equation. We find the maxima and minima in the absorption of the applied electric field shift when the Coulomb interaction is included. We then use the calculated absorption with the drift–diffusion equations to calculate the responsivity in a partially depleted absorber (PDA) photodetector, and we obtain excellent agreement with experiments at all biases and optical wavelengths.

OCIS codes: (040.5160) Photodetectors; (060.5625) Radio frequency photonics.

http://dx.doi.org/10.1364/OL.41.000456

High-current photodetectors play an important role in RF-photonics links [1] and in photonic microwave generation [2]. Recent work has shown that the Franz–Keldysh effect is an important source of nonlinearity in high current photodetectors [3–5]. The absorption coefficient oscillates when the incident light wavelength or the electric field changes. Recent work [6–8] has also demonstrated that the responsivity of high-current, partially depleted photodetectors (PDAs) or uni-traveling carrier photodetectors (UTC) oscillates as the photon energy changes due to the Franz–Keldysh effect [9]. However, work to date has used an analytical formula for the absorption due to the Franz–Keldysh effect that does not include the Coulomb interaction [3,8,10]. This formula does not always yield good agreement with experiments since the Coulomb interaction shifts the maxima and minima of the responsivity. It is important to obtain accurate results for the impact of the Franz–Keldysh effect on high-current photodetectors since it is often the most important physical effect limiting a high-current photodetector's linearity and responsivity. In prior work, we [4,5] showed that the Franz–Keldysh effect must be included to accurately model a PDA photodetector, but we did not include the Coulomb interaction. In this Letter, we include the Coulomb interaction [11,12] in the calculation of the absorption coefficient of a PDA photodetector to calculate the responsivity using the drift–diffusion equations [4,5,13,14]. We show that the Coulomb interaction must be included in the model to obtain good agreement with experiments at all optical wavelengths.

The expression for the absorption coefficient α [15,16] in the effective mass approximation is (in SI units)

$$\alpha = \frac{2\pi e^2}{m_0^2 \epsilon_0 c \eta' \omega} |U(0)|^2 |\langle c\mathbf{k}_0 | \mathbf{e}\cdot\mathbf{p} | v\mathbf{k}_0\rangle|^2 S(\hbar\omega), \tag{1}$$

where e is the magnitude of the electron charge (here positive), m_0 is the electron mass, ϵ_0 is the vacuum permittivity, η' is the real part of the refractive index at the angular frequency ω, c is the speed of light, $U(\mathbf{r})$ is the solution of the effective mass equation as a function of the relative coordinate $\mathbf{r}$, $\mathbf{k}_0$ is the point in $\mathbf{k}$ space where the minimum energy gap between the conduction band c and the valence band v occurs, $\mathbf{e}\cdot\mathbf{p}$ denotes the matrix elements of the transition, and $S(\hbar\omega)$ is the density of excited states at the photon energy $\hbar\omega$ above the ground state. The effective mass equation that governs the relative motion of an electron-hole pair is

$$\left(-\frac{\hbar^2}{2m^*}\nabla^2 - \frac{e^2}{4\pi\epsilon_0\epsilon_r r} + eFx\right) U(r) = EU(r), \tag{2}$$

where m^* is the effective mass, ϵ_r is the relative permittivity of the material, F is the electric field and is taken to be in the x direction, and $E = 0$ corresponds to the gap energy E_g. The second term on the left is due to the Coulomb interaction between an electron and a hole. If we neglect this term, then the solution of Eq. (2) can be expressed in terms of Airy functions [17].

If units are chosen so that both the exciton Rydberg energy,

$$R = \frac{m^* e^4}{2\hbar^2 (4\pi\epsilon_0\epsilon_r)^2}, \tag{3}$$

and the exciton Bohr radius,

$$a = \frac{4\pi\hbar^2\epsilon_0\epsilon_r}{m^* e^2}, \tag{4}$$

are unity, then the effective mass equation becomes

$$\left(-\nabla^2 - \frac{2}{r} + fx\right) U = EU, \tag{5}$$

where the field strength f is measured in units of (Rydbergs)/[(Bohr radius)-(electron charge)]≡ Rbe.

Equation (5) is not separable in spherical polar coordinates, but it is separable in parabolic coordinates defined by

$$\xi = r + x, \qquad \zeta = r - x, \qquad \phi = \phi. \tag{6}$$

The solution of Eq. (5) may be written in the form [12,18]

$$U(r) = \frac{\chi_1(\xi)\chi_2(\zeta)\exp(im\phi)}{(\xi\zeta)^{1/2}}, \tag{7}$$

where m is the angular quantum number. Substituting Eq. (7) into Eq. (5) and separating the variables ξ and ζ, we obtain

$$\chi_1''(\xi) + \left(\frac{1-m^2}{4\xi^2} + \frac{\rho}{\xi} + \frac{E}{4} - \frac{f\xi}{8}\right)\chi_1(\xi) = 0, \tag{8a}$$

$$\chi_2''(\zeta) + \left(\frac{1-m^2}{4\zeta^2} + \frac{1-\rho}{\zeta} + \frac{E}{4} + \frac{f\zeta}{8}\right)\chi_2(\zeta) = 0, \tag{8b}$$

where $\chi_1''(\xi)$ denotes $d^2\chi_1(\xi)/d\xi^2$, $\chi_2''(\zeta)$ denotes $d^2\chi_2(\zeta)/d\zeta^2$, and ρ is a separation parameter. When we do not include the Coulomb interaction in the effective mass equation, we can still separate Eq. (5). The only difference is that we must replace $1-\rho$ with $-\rho$ in Eq. (8b). We use a Numerov integrator [19] to solve these equations [11,12]. We then obtain the absorption coefficient

$$\alpha = \left(\frac{2\pi e^2}{m_0^2\epsilon_0 c\eta'\omega}\right)\left(\frac{|\langle c\mathbf{k_0}|\mathbf{e}\cdot\mathbf{p}|v\mathbf{k_0}\rangle|^2}{A^2\pi^2 f^{1/2}\int_0^\infty[\chi_1^2(\xi)/\xi]\mathrm{d}\xi}\right), \tag{9}$$

where A is a coefficient that can be determined by solving the differential Eq. (8b) [11,12]. The effect of the Coulomb interaction on the absorption appears through its effect on this parameter. We define a normalized absorption coefficient

$$\tilde{\alpha} = |U(0)|^2 S(\hbar\omega) = \frac{1}{A^2\pi^2 f^{1/2}\int_0^\infty[\chi_1^2(\xi)/\xi]\mathrm{d}\xi}. \tag{10}$$

In calculating the responsivity of the photodetector, it is usual to assume that the responsivity factor $|\langle c\mathbf{k_0}|\mathbf{e}\cdot\mathbf{p}|v\mathbf{k_0}\rangle|^2$ is not known a priori. Hence, it is standard to treat it as a fitting parameter to obtain the best agreement possible with experiments [3]. We will show that even with this assumption it is not possible to obtain good agreement over a range of optical wavelengths without including the Coulomb interaction. Additionally, this approach makes definite predictions for the responsivity factor with and without the Coulomb interaction that can be compared to prior calculations [20,21]. We will show that including the Coulomb interaction leads to significantly better agreement with the prior calculations.

We use the drift–diffusion equations to model the PDA photodetector [22], which have been modified to include the following effects: (1) field-dependent mobilities and diffusion coefficients for both holes and electrons, (2) a history-dependent impact ionization, and (3) the Franz–Keldysh effect. We show the structure of the PDA photodetector in Fig. 1.

The model consists of three equations that govern the dynamics of the electron density n, the hole density p, and the electric field $\mathbf{F}$ (negative gradient of the electrostatic potential, φ):

$$\frac{\partial(n - N_D^+)}{\partial t} = G_i + G_L - R(n,p) + \frac{\nabla\cdot\mathbf{J}_n}{e}, \tag{11a}$$

$$\frac{\partial(p - N_A^-)}{\partial t} = G_i + G_L - R(n,p) - \frac{\nabla\cdot\mathbf{J}_p}{e}, \tag{11b}$$

$$\nabla\cdot\mathbf{F} = \frac{e}{\epsilon}(N_D^+ + p - n - N_A^-), \tag{11c}$$

where G_i and G_L are the impact ionization and photon generation rates, R is the recombination rate, ϵ is the permittivity of the semiconductor material, and N_D^+ and N_A^- are the ionized donor and acceptor impurity concentrations. The variables $\mathbf{J}_n$ and $\mathbf{J}_p$ are the current densities for electrons and holes.

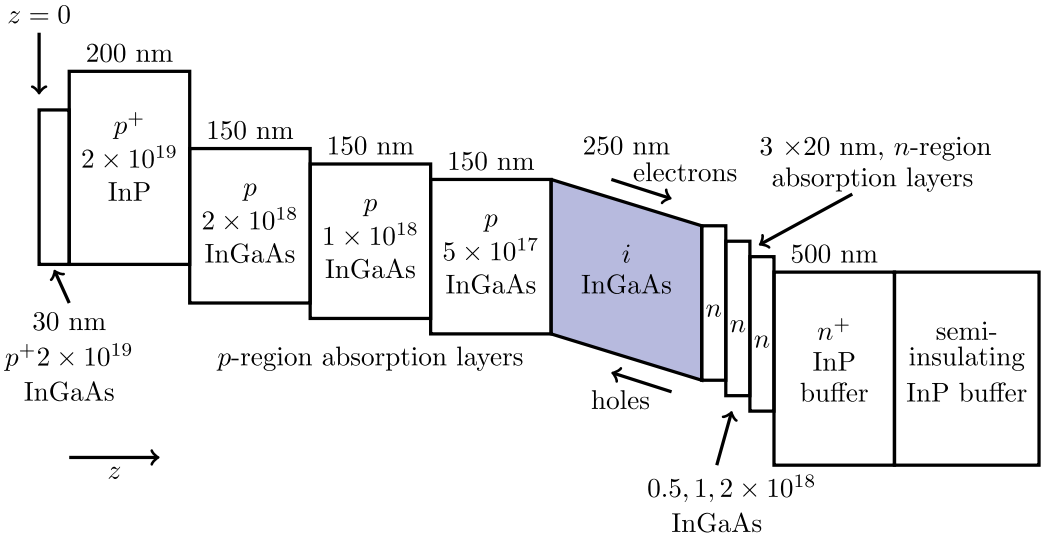

Fig. 1. Structure of the PDA photodetector. The Franz–Keldysh effect is only important in the i-layer, shown in blue.

The photon generation rate is given by [23]

$$G_L(z) = Q\alpha(\omega, F)\exp[-\alpha(\omega, F)(L_{ab} - z)], \quad (12)$$

where Q is the incident photon flux entering the device, $\alpha(\omega, F)$ is the absorption coefficient as a function of the incident light angular frequency ω and the magnitude of the electric field F, L_{ab} is the length from the p-region to the end of the n-region absorption layers, and z is the position in the device from the left (Fig. 1). The Franz–Keldysh effect appears in the drift–diffusion equations by first affecting the absorption coefficient α as described by Eq. (9) which, in turn, affects the photon generation rate G_L as described by Eq. (12), which then appears in Eqs. (11a) and (11b). In the simulations, we only consider single-pass illumination, and we do not consider interface reflection. The reflection coefficient between the InP and InGaAs layers is 0.022, which may slightly impact the responsivity but will not change the responsivity as a function of bias. We include Shockley–Read–Hall recombination, Auger recombination, and radiative recombination. We use a finite difference method to solve the equations, and we use thermionic boundary conditions at the interfaces. More details on the model may be found in [13,14].

Figure 2 shows the normalized absorption coefficient $\bar{\alpha}$, defined in Eq. (10), as a function of electric field with and without the Coulomb interaction in $In_{0.53}Ga_{0.47}As$. The dashed and solid curves are the simulation results with and without the Coulomb interaction, respectively. We show the material parameters that we used in the calculation in Table 1. We find that the amplitude of the normalized absorption coefficient $\bar{\alpha}$ is larger by approximately a factor of two when we include the Coulomb interaction in the calculation. Since the responsivity factor $|\langle c\mathbf{k_0}|\mathbf{e}\cdot\mathbf{p}|v\mathbf{k_0}\rangle|^2$ is assumed to be unknown and is determined from a best fit to the measured responsivity, this factor of two difference is not important when comparing the theoretically calculated responsivity as a function of bias and optical wavelength to the measured values. What is important is the difference in the slope between these two calculations. For an electric field between 50 and 100 Rbe, the slope with the Coulomb interaction is larger than without. In both calculations, the oscillations become more rapid as the field diminishes, but the values at which the minima and maxima occur are different, as are the oscillation periods.

Table 1. Material Parameters at 300 K Used in the Simulation[a]

Parameter	$In_{0.53}Ga_{0.47}As$
E_g(eV)	0.73
ϵ_r	13
m_e^*/m_0	0.041
m_{hh}^*/m_0	0.59
m_{lh}^*/m_0	0.051
m^*/m_0	0.031
R(eV)	0.0025
a(m)	2.22×10^{-8}

[a] m_0 is the electron mass.

We show the responsivity as a function of bias for different wavelengths in Fig. 3. When the bias is between 1 and 5 V, the electric field is between 4×10^6 and 2×10^7 V/cm, which corresponds to 36–180 Rbe. Without the Coulomb interaction in the simulation, we cannot obtain agreement at 1560 and 1580 nm, even with an optimal choice of the responsivity factor. When the Coulomb interaction is not included, we see in Fig. 2 that the absorption coefficient first decreases and then becomes flat for an electric field between 50 and 150 Rbe. Hence, the responsivity first decreases and then begins to increase at the wavelengths $\lambda = 1560$ and $\lambda = 1580$ nm due to the impact ionization. By contrast, when the Coulomb interaction is included, the absorption coefficient always decreases for an electric field between 50 and 100 Rbe. Thus, the simulated responsivity decreases as the field increases, which agrees with experiments.

While the responsivity factor $|\langle c\mathbf{k_0}|\mathbf{e}\cdot\mathbf{p}|v\mathbf{k_0}\rangle|^2$ is assumed unknown and plays no role in our calculation of the responsivity, our simulations, combined with the experimental measurements of the responsivity, make definite predictions for this factor. Without the Coulomb interaction, we predict $|\langle c\mathbf{k_0}|\mathbf{e}\cdot\mathbf{p}|v\mathbf{k_0}\rangle|^2 = 3.11\times10^{-48}$ J-s and, with the Coulomb

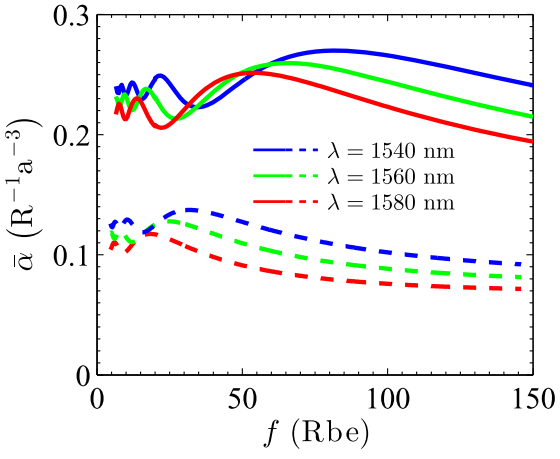

Fig. 2. Calculated absorption coefficient as a function of electric field. The solid curves show the calculation results with the Coulomb interaction, and the dashed curves show the calculation results without the Coulomb interaction, using Eq. (10).

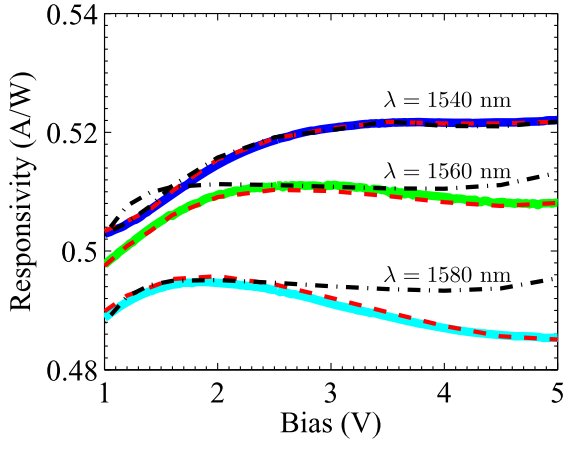

Fig. 3. Calculated and measured responsivity as a function of bias. The solid curves show the experimental results, the dashed curves show the simulation results with the Coulomb interaction, and the dashed-dotted curves show the simulation results without the Coulomb interaction.

interaction, we predict $|\langle c\mathbf{k_0}|\mathbf{e}\cdot\mathbf{p}|v\mathbf{k_0}\rangle|^2 = 1.40\times10^{-48}$ J-s. This transition matrix element can be calculated using the procedure that is described in [20] and is approximately 1.51×10^{-48} J-s [21], which provides a further verification of the importance of the Coulomb interaction.

In conclusion, we have theoretically investigated the impact of the Coulomb interaction on the Franz–Keldysh effect in high-current PDA photodetectors. The Franz–Keldysh effect is the most important effect limiting the linearity of these devices and leads to oscillations in the responsivity. We proceeded by using the Franz–Keldysh effect, both with and without the Coulomb interaction, to determine the absorption coefficient in the *i*-region of the device, and we then used this absorption coefficient in the drift–diffusion equations to calculate the responsivity. We found that it is necessary to take into account the Coulomb interaction in order to obtain agreement with experiments at all optical wavelengths and biases.

Funding. Naval Reseach Laboratory (N00173-09-2-C016, N00173-15-1-G905).

Acknowledgment. The authors would like to thank T. F. Carruthers for useful discussions. The simulations were carried out at UMBC's high performance computing facility.

REFERENCES

1. V. J. Urick, F. Bucholtz, J. McKinney, P. S. Devgan, A. L. Campillo, J. L. Dexter, and K. Williams, J. Lightwave Technol. **29**, 1182 (2011).
2. T. M. Fortier, F. Quinlan, A. Hati, C. Nelson, J. A. Taylor, Y. Fu, J. Campbell, and S. A. Diddams, Opt. Lett. **38**, 1712 (2013).
3. Y. Fu, H. Pan, Z. Li, A. Beling, and J. C. Campbell, IEEE J. Quantum Electron. **47**, 1312 (2011).
4. Y. Hu, C. Menyuk, M. Hutchinson, V. Urick, and K. Williams, in *Photonics Conference (IPC)* (IEEE, 2014), pp. 206–207.
5. Y. Hu, T. F. Carruthers, C. R. Menyuk, M. N. Hutchinson, V. J. Urick, and K. J. Williams, Opt. Express **23**, 20402 (2015).
6. A. S. Hastings, D. A. Tulchinsky, K. J. Williams, H. Pan, A. Beling, and J. C. Campbell, J. Lightwave Technol. **28**, 3329 (2010).
7. M. Schmid, M. Kaschel, M. Gollhofer, M. Oehme, J. Werner, E. Kasper, and J. Schulze, Thin Solid Films **525**, 110 (2012).
8. K. Takeda, T. Hiraki, T. Tsuchizawa, H. Nishi, R. Kou, H. Fukuda, T. Yamamoto, Y. Ishikawa, K. Wada, and K. Yamada, IEEE J. Sel. Top. Quantum Electron. **20**, 64 (2014).
9. L. V. Keldysh, Sov. Phys. JETP **7**, 788 (1958).
10. D. J. Hall, T. J. C. Hosea, and D. Lancefield, J. Appl. Phys. **82**, 3092 (2001).
11. H. I. Ralph, J. Phys. C **1**, 378 (1968).
12. J. D. Dow and D. Redfield, Phys. Rev. B **1**, 3358 (1969).
13. Y. Hu, C. Menyuk, V. Urick, and K. Williams, in *2013 International Topical Meeting on Microwave Photonics (MWP)*, Alexandria, VA, Oct. 28, 2013, pp. 282–285.
14. Y. Hu, B. Marks, C. Menyuk, V. Urick, and K. Williams, J. Lightwave Technol. **32**, 3710 (2014).
15. R. J. Elliott, Phys. Rev. **108**, 1384 (1957).
16. C. Hamaguchi, *Basic Semiconductor Physics* (Springer, 2009).
17. K. Tharmalingam, Phys. Rev. **130**, 2204 (1957).
18. L. D. Landau and E. M. Lifshitz, *Quantum Mechanics* (Pergamon, 1958).
19. J. Q. Gonzalez and D. Thompson, Comput. Phys. **11**, 514 (1997).
20. J. Taylor and V. Tolstikhin, J. Appl. Phys. **87**, 1054 (2000).
21. E. Zielinski, H. Schweizer, K. Streubel, H. Eisele, and G. Weimann, J. Appl. Phys. **59**, 2196 (1986).
22. D. A. Tulchinsky, X. Li, N. Li, S. Demiguel, J. C. Campbell, and K. J. Williams, IEEE J. Sel. Top. Quantum Electron. **10**, 702 (2004).
23. S. M. Sze and K. K. Ng, *Physics of Semiconductor Devices*, 3rd ed. (Wiley, 2007).